Russian Geology and Geophysics
Vol. 43, No. 1, pp. 56-64, 2001

Geologiya i Geofizika
UDC 550.42+548.32:549.(324.31+283)

DETERMINATION OF BINDING FORMS OF GOLD IN PYRITE BY MEANS OF STATISTICAL ANALYSIS

V. L. Tauson, O. I. Bessarabova, R. G. Kravtsova, T. M. Pastushkova, and N. V. Smagunov

Vinogradov Institute of Geochemistry, Siberian Branch of the RAS, 1a ul. Favorskogo, Irkutsk, 664033, Russia

Experiments show that the concentration of lattice gold can be estimated against the bulk Au content dominated by adsorbed gold using extrapolation of the concentration of uniformly distributed Au vs. mean specific surface area of crystal dependence onto the region where the effect of surface is negligible. The optimum mean specific surface area for gold in pyrite is 6 cm^2/g. This approach is applicable to natural minerals as well. Comparison of synthetic and natural pyrite from Au-Ag deposits and occurrences in northeastern Russia shows that almost all uniformly distributed (invisible) gold in pyrite is due rather to sorption than to incorporation of Au into the mineral structure, and gold uptake in both cases is driven by one and the same mechanism related to reactivity of defect sites on crystal surface. High concentrations of invisible gold in pyrite are due to Au^0 particles and, possibly, more complicated metastable Au-bearing phases produced by decomposition of intermediate compounds and complexes of Au and gold guide elements (primarily, As) that adsorb on crystal surfaces.

Gold, binding forms, synthesis of minerals, crystals, pyrite, specific surface area

INTRODUCTION

High concentrations of gold in pyrite remain hitherto poorly explained in spite of active experimental efforts [1–7]. Before the SIMS (Secondary Ion Mass Spectrometry) and PIXE (Particle Induced X-ray Emission) methods appeared, this blind spot had been attributed to low analytical precision, which did not allow discrimination among binding forms of invisible gold. More evidence has been reported lately that high Au contents may be due to its lattice-bound or another form distributed in minerals as evenly as lattice gold. The nature of the latter remains disputable [5, 8, 9], and the available estimates of its concentration vary from tens [10] to hundreds or even thousands ppm [5, 8, 11]. EMPA was applied to prove the existence of specific nonmineral Au in pyrite [11] shown by electron- and ion microprobes as homogeneously distributed Au [4, 6]. At the same time, gold solubility in pyrite at 500 °C and 1 kbar is as low as 3±1 ppm, which also holds for high-As systems most often associated with high Au concentrations in natural pyrite [6, 7]. This is well consistent with Au partitioning among its natural concentrators [12] indicating that the limit concentration of gold in natural pyrite never exceeds ~5 ppm. The true between coefficient of Au partitioning pyrite and fluid being quite low [6], the ultra-high concentration of gold in pyrite, viewed formally, must indicate its fairly high contents (thousands or tens of thousands ppm) in fluids. However, according to data on gold solubility and complexing [13, 14], these high concentrations can hardly be effectuated in natural conditions, except for some exotic solutions [15]. Therefore, there must be some particular conditions that favor the predominant formation of lattice gold, such as crystallization from strongly supersaturated fluids producing crystals in which gold is incorporated in a different manner than into defect-free pyrite [3]. On the other hand, we should not *a priori* exclude the existence of natural conditions responsible for high gold concentrations. In this context natural high-Au fluids would be of particular interest as active gold carriers highly sensitive to the chemical environment (especially, pH and reduced S concentrations). However, the problem can be formulated in such a way only for lattice gold which is amenable to Henry's law.

Discrimination among forms of invisible gold is a fairly difficult task, which hitherto eluded unambiguous solution by the existing methods. SIMS, though being the most suitable techniques [6, 7], cannot directly detect

lattice gold [8] but can only indicate that some portion of the Au impurity is distributed as homogeneously. As for the PIXE method and ion channeling techniques, only few examples are known [8] and only very preliminary conclusions can be drawn. Anyway, the application of these methods (as well as Mössbauer spectroscopy of ^{197}Au and ESR) has been so far restricted to natural pyrite with unknown binding forms of gold [16–18], and their calibration remains problematic.

We suggested a quite simple method for discrimination between Au binding forms [6, 7] based on statistical analysis of crystals of gold-bearing minerals. The basic postulate in this method is that trace elements in various single crystals in a representative assemblage exist in different forms depending on the type and number of defects in a crystal, development of its surface, growth rate, etc. Therefore, there is a probability, depending on specific mineral-forming conditions, that a crystal may contain a trace element in a lattice or a non-lattice form. In other words, any representative assemblage always includes several crystals free from active sites or defects and thus responsible for the presence of non-lattice constituents. As all these obviously enhance the bulk content of the trace element, the task is to obtain a statistical sample of single crystals that contain it in minor but significant (above detection limit) amounts. Best suitable for discrimination of lattice gold is a sample of minimum concentrations with a coefficient of variation under 20% (without random error) [19]. The procedure of statistical data processing for single crystals containing lattice gold includes the following steps: (1) to outline an initial sample (n_1) of minimum Au concentrations (1/3 of the total assemblage of N crystals, most often $N = 20$) that are at least 3 times the detection limit; (2) to find average x_1 over the sample and then make up a new (final) sample n_2 by adding values that depart from x_1 for no more than 30% (the aforementioned 20% plus 10% of analytical error) and excluding those that depart for more than +30%; (3) for the final sample to find the mean x_2 and the mean standard error ($\pm\sigma$, considered analytical uncertainty) in the concentration of lattice gold. Note that the variability in the final sample may exceed 30%, as the minimum Au concentrations are not excluded if determined reliably even when they fall outside the 30% bar, which may occur both at very low and very high gold contents [19]. Samples in these extreme cases may be poorly representative statistically but not always can be enlarged because of unsuitable quality of crystals.

Note again that the statistical methods for discrimination of lattice gold can only indicate that some portion of gold is distributed in the same manner as lattice Au. However, the lattice-bound impurity can be constrained more rigorously in experiments, on the basis of its distribution in a system for which this impurity is known to enter at least one mineral structure (reference mineral) [6, 7]. Thus, having filtered the noise, one may then check if Au constituent (signal) fits the general distribution of lattice-bound impurities, i.e., the principle of phase composition correlation and Henry's law. For this the experiments are carried out at different Au activities in a system defined by gold guide elements (GGE) [6, 7], with a special focus on the region of Au undersaturation in which lattice gold can be more easily discriminated [19].

However, in this form the method is poorly applicable to the problem of ultra-high Au concentration in natural pyrite for several reasons. First, it requires high-quality facetted crystals free from surface defects and big enough to contain sufficient amount of gold. Second, lattice gold cannot be statistically discriminated from homogeneously distributed gold produced by sorption of Au^0 or Au complexes and intermediate GGE-Au compounds on crystal surface, as it was shown by analysis of crystals in the region of mineral Au saturation (which is of interest in the context of high-Au natural pyrite) [4, 7]. This portion of evenly distributed gold constituent can be separated as a component proportional to the specific surface area of a crystal [6]. In this case natural pyrite, for which the limit concentration of Au is unknown, should be replaced by synthetic pyrite and the results then compared with those for natural minerals. Finally, it is hard to prove that the discriminated constituent is true lattice gold, and this is the only problem the discussed method cannot solve unambiguously for natural minerals. However, the significance of this problem depends upon the importance of lattice-bound gold: If analysis shows non-lattice gold to be the predominant form, it should be considered a solution to the high-Au pyrite problem, but then additional investigation may be needed to gain information on Au concentrations in the ore-forming fluid.

METHODS

In this study, Au concentration was determined by atomic absorption spectrometry (AAS) using graphite furnace techniques after acid dissolution of each crystal. Analyses were carried out using an AAS Perkin-Elmer M 503 spectrometer with a deuterium background corrector and an HGA-74 graphite furnace, under argon flow, at Au detection limit of 0.2 ppb and an uncertainty of ±10%. A hollow cathode lamp (made in Russia) was used as a light source, and signal amplitudes were recorded by a Hitachi 056 potentiometric recorder. For more detail of the procedure see [19]. The task to pick crystals with minor Au contents from small single crystals (0.1–5 mg) requires a standard in which the distribution of the analyzed element is uniform and reproducible even in such

Table 1

Gold in Dissolved Au-bearing (45±7 ppm) CdS Standard

Conc. Au added, μg/l	Conc. Au found, μg/l		
	Fresh solution	Day old solution	10 day old solution
Dissolved in HCl			
13.1	12.0	8.3	8.4
5.2	4.8	2.1	4.5
2.6	2.8	1.4	1.1
1.3	1.4	0.5	0.8
0.35	0.3	0.1	0.1
Dissolved in aqua regia			
12.8	12.0	7.0	9.5
5.1	7.0	2.2	7.4
3.1	4.3	1.3	2.3
1.3	1.3	0.7	0.8
0.3	0.3	<0.2	0.4
Dissolved in HCl + NaCl			
9.3	8.8	7.9	7.4
3.9	3.8	3.5	2.4
1.9	1.9	1.6	0.6
1.0	1.2	0.9	1.0
0.4	0.5	0.3	0.2

small specimens. This standard is necessary in analytical data modeling for small single crystals, methodological investigations, estimation of detection limit, and testing in order to reveal statistically significant minimum concentrations.

The available 2 to 30 mg standards of galena GF-1, sphalerite SF-1, and pyrite PS-1 (Freiberg, Germany) turned to be inapplicable in our case, as Au concentrations in them showed a strong and irregular weight dependence. Therefore, we used greenockite (α-CdS) synthesized hydrothermally in the region of Au undersaturation in the CdS–PbS–NH_4Cl–H_2O system, with As as a GGE, at 500 °C and 1 kbar, containing 45±7 ppm Au, of which 41±4 ppm was distributed uniformly in the same manner as lattice gold [6, 7]. Au distribution was analyzed by the above method either after decomposition of crystals in HCl or aqua regia, or by the direct method (in solid specimens) using an AAS EA5 spectrometer [19]. Specimens of 10–15 mg (20–30 grains) of the standard are sufficient to provide good reproducibility. The basic solution was then diluted to make solutions with Au concentrations from 0.3 to 13 μg/l (Table 1). Fresh solutions of 99.999% metallic gold in HCl were used as calibration standards. Irrespective of the way of preconditioning, the 0.3–13 μg/l solutions were stabilized by adding $\sim 10^{-4}$ wt.% NaCl, otherwise up to 60% Au could be lost after 24 hours because of the instability of the $AuCl_3$ solution [20] (Table 1). The Au detection limit for fresh solutions is at least 0.3 μg/l (0.3 ppb) (Table 1), and the precision is in average ±12%. It is somewhat higher for crystals dissolved in HCl (±9–11%) but the available evidence is insufficient to give preference to this solvent. The best solvent for pyrite is HCl + $KClO_3$. In all cases measurements were taken in fresh solutions.

RESULTS

Synthetic pyrite. Pyrite crystals were hydrothermally synthesized in the system Fe–S–CdS–As–Au–NH_4Cl–H_2O at 500 °C and 1 kbar. For details of the experimental procedure see [6, 7]. This consideration is restricted to one successful experiment which yielded a lot of pyrite crystals of similar shapes and of various sizes (mean

Table 2

Gold in Five Samples of Synthetic Pyrite of Various Crystal Sizes Synthesized in System Fe–S–CdS–As–Au–NH_4Cl–H_2O, with 1 wt.% As, at 500 °C and 1 kbar

Initial sample (N)				Final sample (n_2)				
Nos.	Number of crystals	Size of crystal, mm*	$\bar{C}_{Au}$, ppm	C_{Au}, ppm	Mean size of crystal ($\bar{r}$), mm**	Mean specific surface area of crystal ($\bar{S}_{sd}$), cm^2/g	$\bar{x}_2 \pm \sigma$, ppm	Percentage of obscuring Au, %
1	18	1.1–1.6	9.1	1.8; 5.1; 3.6; 4.4	1.433	4.38	3.7 ± 1.7	23
2	19	0.8–1.1	10.3	4.4; 4.8; 2.4; 4.8; 4.3	1.104	8.15	4.1 ± 1.4	27
3	20	0.6–0.8	20.7	5.3; 8.9; 6.9; 5.4; 6.5	0.747	12.03	6.6 ± 2.1	55
4	20	0.3–0.6	40.2	15.5; 12.4; 11.0; 15.5; 10.0; 2.5	0.574	15.70	11.2 ± 5.5	73
5	20	0.2–0.4	80.9	9.7; 9.0; 17.6; 19.0; 14.4	0.463	19.42	13.9 ± 6.5	78

* Measured as radius of approximating hemisphere.
** Calculated from mean weight of crystals approximated by hemisphere.

effective diameters from 0.4 to 3.0 mm). The crystals were synthesized in the presence of 1% As (0.01 wt.% bulk content) used as GGE and contained in average 6.2±2.0 ppm of uniformly distributed Au. The crystals were of pentagon-dodecahedron shapes or octahedrons in various combinations with cube and rhomb-dodecahedron, or less often with trigonal and tetragonal octahedrons. Because of numerous small faces and surfaces of contact with the Ti closure of pressure vessel, the crystals had intricate shapes and looked like hemispheres. The morphology of the crystals is controlled by the As impurity and their geometry follows the concave hemisphere of the closure piece. The various sizes of the crystals are defined by the distance from the nucleation points to the top of the hemisphere where supersaturation is the highest. As it was impossible to account for the real shape of each crystal, it was approximated by a hemisphere of radius r. The crystals were divided into five groups according to their sizes (Table 2); if necessary, their surfaces were cleaned from quenching phases mechanically (under glycerol). We tried to use crystals with clear faces free from surface overgrowths and contamination, 20 crystals from each size fraction. The results are given in Table 2 which shows the bulk Au content increasing with decreasing sizes of crystals. The average size of crystals $\bar{r}$ corresponding to the C_{Au} values in the final sample of minimum concentrations (n_2, see above) was determined on the basis of the mean weight of hemisphere-approximated crystals; then the average specific surface area of crystals of each size group was calculated as $\bar{S}_{sp} = 3\pi\bar{r}^2/\bar{m}$, where $\bar{m}$ is the mean crystal weight in the n_2 sample. The concentration of homogeneously distributed Au strongly depends on the specific surface area of an average crystal (Table 2). Taking into account that the limit concentration of Au in pyrite in these conditions is about 3 ppm [6, 7], this relationship can be expressed as a nearly parabolic curve (Fig. 1). Since $\bar{x}_2$ is expected to grow again in the region of very small specific surfaces (see below), the relationship is given by

$$\bar{x}_2 = -0.006\bar{S}_{sp}^3 + 0.25\bar{S}_{sp}^2 - 2.41\bar{S}_{sp} + 9.98$$

where $\bar{x}_2$ is in ppm, and $\bar{S}_{sp}$ is in cm^2/g. According to this equation, pyrite crystals with better developed surfaces (20 to 40 cm^2/g), typical of natural pyrite (Table 3), may contain 14–70 ppm of uniformly distributed adsorbed gold, which is consistent with our observations (see the following section).

The proportion of adsorbed gold that obscures lattice gold increases as $\bar{S}_{sp}$ grows from 23 to 78%. The

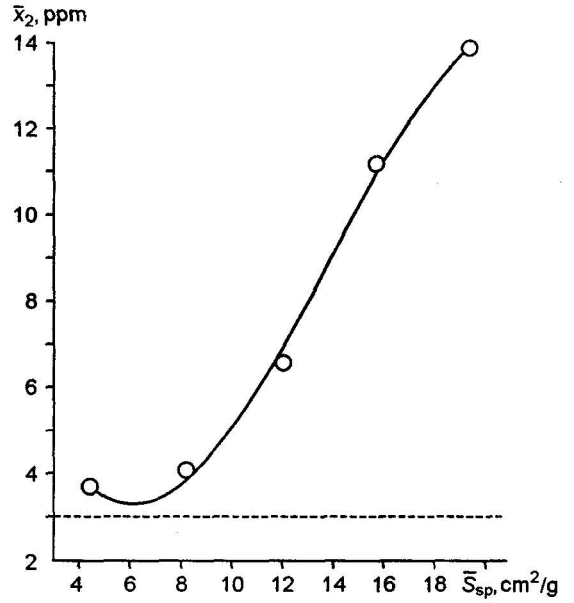

Fig. 1. Concentration of uniformly distributed Au in synthetic pyrite ($\bar{x}_2$ in final sample of minimum values, n_2) plotted against mean specific surface area of crystals. Dashed line shows limit concentration of Au in pyrite at T = 500 °C and P = 1 kbar.

sorption effect can be considered negligible only at $\bar{S}_{sp}$ ~6 cm^2/g (Fig. 1). Recalculation of this value onto the mean effective diameter of crystals yields 2.25 mm. Note that a similar value (2±0.5 mm) was recommended in [21] as optimum for the sample of crystals with the least concentrations of adsorbed gold.

Thus, the study of synthetic gold-bearing pyrite shows that lattice gold can in principle be discriminated even at high Au contents and despite the obscuring effect of non-lattice gold by extrapolation of the $\bar{x}_2$ vs. specific surface area curve onto the region of low $\bar{S}_{sp}$ (at best to 6 cm^2/g).

Natural pyrite. We studied pyrite from ore veins in Au-Ag deposits (Dal'nee, Kvartzevoye) and the Oroch gold occurrence (northeastern Russia) located within the Even tectonic province, one major structure of the central Okhotsk-Chukotka volcanic belt. These are typical epithermal low-sulfide Au-Ag ores [22, 23] existing as veins or vein-like bodies composed of 90–99% quartz, 5–10% adularia, 1 to 10% sericite, hydromica, carbonates, and kaolinite, and 1–3% ore minerals. The latter are dominated by pyrite and the main phases include proustite, pyrargyrite, argentite, electrum, native gold and silver, polybasite, and gray ores. Of lesser importance are arsenopyrite, galena, sphalerite, chalcopyrite, antimonite, miargyrite, pearceite, and stephanite [24]. Most of the ore minerals, especially pyrite [11, 25], are gold concentrators. Our method turned to be inapplicable to anhedral crystals of high-Au pyrite of the Kvartzevoye deposit (mean Au concentration 240 ppm, maximum 1 wt.%, from analysis of 20 grains). According to our observations, the less perfect are the pyrite crystals the more invisible gold they contain. These crystals are typical of ores formed at shallower depths at relatively low temperatures (<~200 °C), whereas the euhedral crystals are, as a rule, generated at greater depths and at higher temperatures (~300–350 °C). We focused on Au-poorer but higher-quality crystals from the Dal'nee deposit and the Oroch occurrence. Most crystals were of cubic shape with striated faces typical of pyrite. We selected crystals of one predominant shape from each size fraction: cubic in three cases and pentagon-dodecahedron in one case (Table 3). Sometimes, the cubes were superposed with small {hk0} and {110} planes, and the edges were often tortuous. Bulk As varied from 0.01 to 0.25 wt.%, and its binding form was not investigated.

Crystals in each sample were divided into four size fractions making representative assemblages of 15–20 grains [7]. This condition was mostly fulfilled, though not always very exactly (Table 3). The problem was that the crystals of the needed quality were small (0.3–0.5 mm), and the most interesting coarse fraction (>1 mm) was poorly represented. The results were processed in the same way as for synthetic pyrite, taking into account the real geometry of the crystals (Table 3, Fig. 2).

Table 3

Gold in Different Size Fractions of Natural Pyrite from Au-Ag Deposits and Occurrences in Northeastern Russia

Sample	Deposit, ore occurrence	Predominant morphology	Bulk As concentration, wt. %	Initial sample (N)			Final sample (n_2)		
				Number of crystals	Size of crystals, mm*	$\bar{C}_{Au}$, ppm	$\bar{x}_2(\pm\sigma)$, ppm	$\bar{r}$, mm**	$\bar{S}_{sp}$, cm^2/g
R-267	Dal'nee	{100}	0.25	15	~0.2	355	99.8 (83.2)	0.278	43.3
				15	~0.3	195	62.5 (10.2)	0.309	38.7
				15	~0.4	220	61.6 (10.7)	0.355	33.9
				16	~0.5	59	20.4 (7.0)	0.409	29.3
S8-58	Oroch	{100}	0.15	12	0.2–0.25	41	19.1 (11.2)	0.311	38.7
				15	0.3–0.35	32	11.8 (7.4)	0.343	34.9
				17	0.4–0.5	27	11.2 (2.4)	0.401	29.9
				18	0.45–0.6	12	3.3 (3.1)	0.456	26.4
K-24	Oroch	{100}	0.01	14	0.3–0.5	26	13.6 (1.8)	0.409	29.3
				14	0.4–0.5	28	10.0 (6.5)	0.468	25.7
				15	0.5–0.6	64	6.9 (5.2)	0.561	21.4
				18	0.6–0.8	38	4.2 (1.1)	0.731	16.4
R-1953	Dal'nee	{210}	0.028	14	0.1–0.2	97	30.5 (6.7)	0.122	43.9
				15	0.15–0.25	40	16.1 (2.4)	0.174	30.8
				15	0.2–0.3	42	9.5 (4.0)	0.187	28.9
				19	0.3–0.45	50	8.3 (5.8)	0.211	25.7

* Edge of polyhedron.
** Calculated from average weight of crystals of each particular shape.

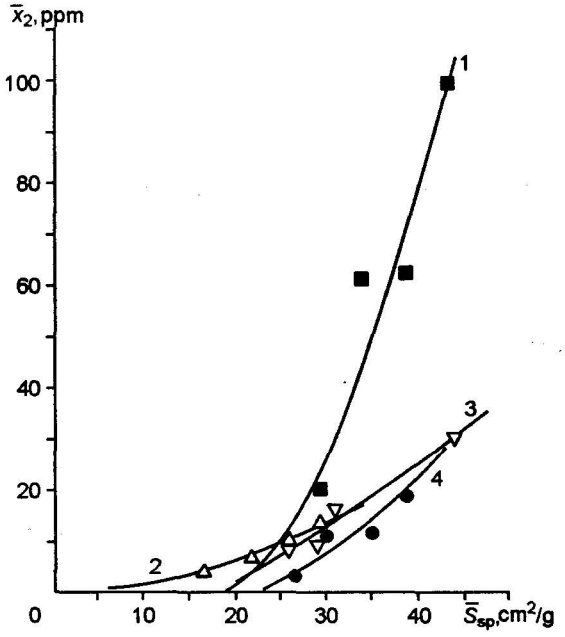

Fig. 2. Concentrations of uniformly distributed Au in natural pyrite plotted against mean specific surface area of crystals in different size fractions (pyrite from Au-Ag deposits in northeastern Russia). Numbers of samples correspond to Table 3: 1 — P-267, 2 — K-24, 3 — P-1953, 4 — C8-58.

DISCUSSION

The dependence of gold concentration on size of the host crystal (or its specific surface area) can be anticipated, as Au^0 particles are attributed to faces and near-surface regions of the crystal under co-crystallization or precipitation of Au with pyrite [1, 3, 26] in synthetic pyrite, unlike some other minerals where invisible gold may occur inside crystals as well [3]. ^{195}Au autoradiography of hydrothermally synthesized pyrite [1] showed that gold is confined to crystal faces and is either disseminated or exists in small particles. The disseminated gold is interpreted either as ultra-fine (<0.5 μm) particles of metallic Au or as adsorbed gold [1]. The same regularity is observed in natural pyrite: INAA applied to coarse pyrite crystals from the Berezovo gold deposit in the Urals [27] showed increasing Au content toward their rims. The presence of gold particles seen under microscope on the rims of coarse pyrite crystals caused doubt about the role of invisible gold in Au distribution. It was also noted that the more uniform the pyrite crystals and grains, the less gold they contain [27].

Au^0 particles and intermediate Au- and GGE-bearing compounds adsorbed on grain surfaces and boundaries in anhedral hydrothermal pyrite may also obscure lattice gold [4, 6], but their appearance on crystal surfaces is likewise controlled by reactivity of defect sites of the growing crystal. The active sites take up components of the growth medium [28], which leads to contamination of the growing surface and decreases the growth rate to termination [29]. Therefore, small crystals in the experiment may have remained so because their growth was inhibited by contamination with Au impurity, including the uniformly distributed Au obscuring lattice gold (Table 2). Note that natural pyrite crystals (Table 3) with more surface defects contain higher concentrations of gold [30]. This means that entrapment of gold occurs in both cases by the same mechanism related to reactivity of defect sites on crystal surfaces. In this context the relationship between the concentration of uniformly distributed gold and the specific surface area of crystals (Figs. 1, 2) can be accounted for by the fact that starting with some small surface area its role in Au uptake becomes insignificant. The slope of the curves for crystals with well developed surfaces correlates with bulk content of As: the higher the content the greater the role of the surface. This (i) means that As is the very agent responsible for high Au concentrations in the system and (ii) proves valid the earlier inference [6, 7] that As does not participate in the crystallochemical mechanism of Au incorporation into pyrite, as extrapolation of the curves from Fig. 2 onto the optimum surface (6 cm^2/g) results in nearly zero Au content in pyrite irrespective of the content of As. Note that further decrease in $\bar{S}_{sp}$ may fail to cause the corresponding decrease in Au content. Larger crystals (≥3–4 mm) in our experiments are contaminated with non-lattice gold (see above) [6, 21], possibly because the probability for the appearance of surface defects responsible for interaction with the impurity increases proportionally to the surface area (if it becomes large enough). It should be also taken into account that extension of the zone of liquid immiscibility near coarse crystals increase the probability for disequilibrium uptake of impurity particles (and fine crystals) [31]. Thus the optimum conditions of growth for pyrite crystals of optimum size and specific surface area are when crystals grow free of surface active sites or defects responsible for sorption of gold from the fluid. This is confirmed by a study of Au (III) reduction-driven sorption on crystals of ore minerals [21]. Extrapolation of the obtained curves (Fig. 2) onto the optimum surface of 6 cm^2/g shows that almost all homogeneously distributed Au in pyrite is due rather to sorption than to incorporation of gold into the mineral structure. The very species of adsorbed gold remaining unclear, intermediate As compounds and products of their decomposition (small Au^0 particles) appear the most plausible candidates. Therefore, high contents of uniformly distributed Au in pyrite are hardly related to metastable miscibility as is suggested in [8, 32, 33].

It was noted [26] that invisible gold in arsenopyrite forms by reduction-driven sorption; Au^0 particles in pyrite are larger. However, analysis of synthetic and natural minerals (Figs. 1 and 2) shows that homogeneously distributed gold in arsenian pyrite that obscures lattice gold (i.e., actually, invisible gold) is rather due to surface enrichment in As and Au intermediate compounds and products of their decomposition. If deposition is spontaneous and the crystals are too small, the resulting Au concentrations can be rather high: In our case they attained 100 ppm (Fig. 2, Table 3) but may be still higher. If crystals grow freely and clear from impurity as they grow, Au concentration depends on their inner structure. Mosaic crystals may retain (at least partially) on subgrain boundaries the initial adsorbed Au which is hard to discriminate from lattice gold in crystals with a developed mosaic structure. However, if the mosaic structure is poorly developed (as, for instance, in relatively high-temperature hydrothermal pyrite [3]), non-lattice gold can occur only on such defects as grain boundaries, cracks, etc., and can be easily discriminated by the statistical method, as its distribution, like the distribution of the defects, cannot be uniform. Therefore, invisible gold in pyrite results from sorption on crystal surfaces of fine particles of Au^0 and, possibly, metastable Au- and GGE-bearing phases produced by decomposition of Au and GGE (primarily, As) intermediate compounds and complexes. This conclusion confirms the active role of some guide elements in the geochemical history of gold [4]. As for lattice gold in natural pyrite, its content is difficult to estimate because it is too low

against the concentration of non-lattice gold and remote extrapolation of the curves in Fig. 2 is necessary. Crystal assemblages that include coarser grains are more informative. However, preliminary estimates can be obtained from pyrite in the Oroch occurrence (Table 3) which has lower contents of As and uniformly distributed gold ($\bar{x}_2$) and larger crystals (sample K-24). Extrapolation of these data onto $\bar{S}_{sp}$ = 6 cm^2/g (though not very reliable, Fig. 2) shows that the concentration of lattice gold is below ~1 ppm, which does not contradict the limit concentration of Au in hydrothermal pyrite [6, 7]. Comparison of this result with the data in Table 3 allows an inference that lattice gold makes an insignificant portion (1 to 10%) of all uniformly distributed Au. Assuming that the true partitioning coefficient of Au between pyrite and fluid is ~0.06 [6], the concentration of gold in the ore-forming fluid can be roughly estimated at ≤~17 ppm, which corresponds to the upper limit concentration in the liquid phase of fluid inclusions in gold deposits [34, 35]. In general, these solutions are rather enriched than «super-concentrated» which would be the case if all uniformly distributed Au were assumed to be lattice gold.

CONCLUSIONS

The data we obtained allow an inference important for the development of the methods for discrimination of lattice-bound trace elements and for investigation of endocrypty [36]. Lattice-bound impurity can be discriminated by separation of the obscuring uniformly distributed adsorbed element by extrapolation of the concentration vs. specific crystal surface dependence onto the region where the effect of the surface area is negligible. For gold, the optimum mean specific surface area is 6 cm^2/g. For other trace elements, it may vary as a function of content and limit concentration. This method is applicable to natural minerals as well. The example of Au-Ag deposits in northeastern Russia shows that almost all uniformly distributed gold in pyrite (invisible gold) is due rather to sorption and its consequences than to the incorporation of gold into the mineral structure. Preliminary data show that the proportion of lattice gold in small (0.2–0.5 mm) pyrite crystals is no higher than 1 to 10% of the total invisible gold. The predominance of adsorbed gold and the lack of coarse crystals (>1 mm) which, according to experiments, are good for extrapolation, make it difficult to estimate the concentration of lattice-bound Au in natural pyrite. Thus, high concentrations of invisible gold in pyrite are due to fine particles of Au^0 and, possibly, more complex metastable Au-bearing phases produced by decomposition of Au and GGE (primarily, As) intermediate compounds and complexes that adsorb on crystal surfaces.

REFERENCES

1. Mironov, A.G., and V.F. Geletii, ^{195}Au study of gold distribution in synthetic pyrite, *Dokl. AN SSSR*, **241**, 6, 1428-1431, 1978.

2. Kozerenko, S.V., A. M. Tuzova, I. M. Rodionova, et al., A mechanism of formation of disseminated gold in iron sulfides, *Geokhimiya*, **12**, 1706-1714, 1986.

3. Tauson, V.L., A.G. Mironov, N.V. Smagunov, N.G. Bugaeva, and V.V Akimov, Gold in sulfides: state of the art of occurrence and horizons of experimental studies, *Geologiya i Geofizika (Russian Geology and Geophysics)*, **37**, 3, 3-14(1-10), 1996.

4. Tauson, V.L., and N.V. Smagunov, effect of gold-accompanying elements on gold behavior in the Fe-S-aqua solution system at 450 °C and 100 MPa, *Geologiya i Geofizika (Russian Geology and Geophysics)*, **38**, 3, 667-674(706-714), 1997.

5. Fleet, M.E., and A.H. Mumin, Gold-bearing arsenian pyrite and marcasite and apsenopyrite from Carlin Trend gold deposits and laboratory synthesis, *Amer. Miner.*, **82**, 1/2, 182-193, 1997.

6. Tauson, V.L., T.M. Pastushkova, and O.I. Bessarabova, On limit concentration and manner of incorporation of gold in hydrothermal pyrite, *Geologiya i Geofizika (Russian Geology and Geophysics)*, **39**, 7, 932-942 (924-933), 1998.

7. Tauson, V.L., Gold solubility in the common gold-bearing minerals: Experimental evaluation and application to pyrite, *Eur. J. Miner.*, **11**, 6, 937-947, 1999.

8. Besten den, J., D.N. Jamieson, and Ch.G. Ryan, Lattice location of gold in natural pyrite crystals, *Nucl. Inst. Meth. Phys. Res.* **B**, 152, 135-144, 1999.

9. Cabri, L.J., The distribution of trace precious metals in minerals and mineral products, *Miner. Mag.*, **56**, 384, 289-308, 1992.

10. Pratt, A.R., C.H. Huctwith, P.A.W. van der Heide, and N.S. McIntyre, Quantitative SIMS analysis of trace Au in pyrite using the infinite velocity (IV) method, *J. Geochem. Explor.*, **60**, 241-247, 1998.

11. Kravtsova, R.G., and L.A. Solomonova, Gold in pyrites from metasomatic ores of Au-Ag deposits in volcanic provinces of the Northern Okhotsk region, *Geokhimiya*, 12, 1867-1872, 1984.

12. Badalov, S.T., Some scientific problems of geochemistry and mineralogy, *Bull. MVO*, **129**, 2, 118-123, 2000.

13. Benning, L.G., and T.M. Seward, Hydrosulphide complexing of Au(I) in hydrothermal solutions from 150-400 °C and 500-1500 bar, *Geochim. Cosmochim. Acta*, **60**, 11, 1849-1871, 1996.

14. Gibert, F., M.-L. Pascal, and M. Pichavant, Gold solubility and speciation in hydrothermal solutions: experimental study of the stability of hydrosulphide complex of gold (AuHS0) at 350 to 450 °C and 500 bars, *Geochim. Cosmochim. Acta*, **62**, 17, 2931-2947, 1998.

15. Chenberger, D.M., and H.L. Barnes, Solubility of gold in aqueous sulfide solutions from 150 to 350 °C, *Geochim. Cosmochim. Acta*, **53**, 2, 269-278, 1989.

16. Voitsekhovskii, V.N., B.P. Berkovskii, O.A. Yaschurzhinskaya, et al., On the problem of binding forms of invisible gold in aresenopyrite and pyrite, *Izv. vuzov. Tsvetnaya metallurgiya*, 3, 60-65, 1975.

17. Marion, P., M. Monroy, P. Holliger et al., Gold bearing pyrites: A combined ion microprobe and Mössbauer spectrometry approach, in *Source, Transport and Deposition of Metals*, eds. Pagel and Leroy, pp. 677-680, Rotterdam, Balkema, 1991.

18. Zhang Zhenru, Yang Sizue, and Yi Wen. Studies of submicro-gold and lattice-gold in some minerals, *J. Cent.-South Inst. Miner. Met.*, **18**, 4, 355-361, 1987.

19. Tauson, V.L., A. Salikhov, J. Matshullat, et al., A possibility to analytical determination of lattice gold in sulfide minerals, *Geokhimiya*, 2001, *in press*.

20. Ryabchikov, D.I., Quantitative determination of precious metals be potentiometric titration, *Zhurn. Analit. Khimii*, **1**, 1, 47-56, 1946.

21. Tauson, V.L., O.V. Ovchinnikova, O.I. Bessarabova, et al., Distribution of gold deposited under reducing adsorption from $HAuCl_4$ solution on magnetite, sphalerite, and galenite crystals, *Geologiya i Geofizika (Russian Geology and Geophysics)*, **41**, 10, 1480-1483(1427-1430), 2000.

22. Belyi, V.F., *Stratigraphy and structure of the Okhotsk-Chukotka volcanic belt* [in Russian], 171 pp., Nauka, Moscow, 1977.

23. Petrovskaya, N.V., *Native gold* [in Russian], 347 pp., Nauka, Moscow, 1973.

24. Kostyrko, N.Ya., L.N. Plyashkevich, and M.V. Boldyrev, Structure and lithology of mineral fields in the Even mineral province, in *Data on the geology and mineral deposits* [in Russian], ed. O.Kh. Tsopanov, 87-94 pp., Magadan, 1974.

25. Kravtsova, R.G., Geochemical zonation and distribution of main tracer elements of Au-Ag hydrothermal systems (Northeastern Russia), *Geokhimiya*, 2, 202-210, 1977.

26. Maddox, L.M., G.M. Bancroft, M.J. Scaini, and J.W. Lorimer, Invisible gold: Comparison of Au deposition on pyrite and arsenopyrite, *Amer. Miner.*, **83**, 11/12, part 1, 1240-1245, 1998.

27. Chesnokov, B.V., and V.I. Popova, Crystal morphology of pyrite from the Berezovsk gold deposit in the Urals, in *Mineralogy and mineralogical crystallography* [in Russian], ed. G.N. Vertushkov, pp. 43-47, Gornyi Inst., Sverdlovsk, 1971.

28. Guevrement, J.M., D.R. Strongin, and M.A.A. Schoonen, Thermal chemistry of H_2S and H_2O on the (100) plane of pyrite: Unique reactivity of defect sites, *Amer. Miner.*, **83**, 11/12, part 1, 1246-1255, 1998.

29. Glasner, A., and M. Zidon, The crystallization of NaCl in the presence of $Fe(CH)_6^{4-}$ -ions, *J. Crystal. Growth*, **21**, 2, 294-304, 1974.

30. Chanturiya, V.A., A.A. Fedorov, and T.N. Matveeva, Evaluation of technological properties of gold-bearing pyrite and arsenopyrite in different deposits, *Tsvetnye metally*, **8**, 9-12, 2000.

31. Petrovskii, V.A., S.A. Troshev, and M.F. Schanov, *Crystal-medium interaction* [in Russian], 328 pp., Syktyvkar, Komi Inst. of Geology, 1992.

32. Fleet, M.E., P.J. Mac Kean, and J. Barbier, Oscillatory-zoned As-bearing pyrite from stratabound and stratiform gold deposits: An indicator of ore evolution, *Econ. Geol. Monograph*, 6, 356-362, 1989.

33. Arehart, G.B., S.L. Chryssoulis, and S.E. Kesler, Gold and arsenic in iron sulfides from sediment-hosted disseminated gold deposits: Implication for depositional processes, *Econ. Geol.*, **88**, 1, 171-185, 1993.

34. Baranova, N.N., A.B. Volynskii, S.V. Kozerenko, et al., Concentrations and binding forms of Au, Te, Sb, and As in mineral-forming solutions of epithermal Au-S-Te deposits, *Geokhimiya*, 12, 1786-1799, 1995.

35. Baranova, N.N., Z.B. Afanas'eva, G.F. Ivanova, et al., Ore-forming processes at the Olimpiada Au-(Sb-W) deposit (from data on mineral parageneses and fluid inclusions), *Geokhimiya*, 3, 282-293, 1997.

36. Tauson, V.D., Isomorphism and endocrypty: new approaches to study behavior of trace elements in mineral systems, *Geologiya i Geofizika (Russian Geology and Geophysics)*, **40**, 10, 1488-1494(1468-1473), 1999.

Editorial responsibility: G.N. Anoshin

Received 10 January 2001
Accepted 15 May 2001

ISSN 1068-7971

RUSSIAN GEOLOGY AND GEOPHYSICS

ГЕОЛОГИЯ И ГЕОФИЗИКА

1–2

Vol. 43, 2002

Siberian Branch, Russian Academy of Sciences/Novosibirsk